Glycine Hinges with Opposing Actions at the Acetylcholine Receptor-Channel Transmitter Binding Site[S]

Prasad Purohit and Anthony Auerbach

Department of Physiology and Biophysics, SUNY at Buffalo, Buffalo, New York

ABSTRACT

The extent to which agonists activate synaptic receptor-channels depends on both the intrinsic tendency of the unliganded receptor to open and the amount of agonist binding energy realized in the channel-opening process. We examined mutations of the nicotinic acetylcholine receptor transmitter binding site (α subunit loop B) with regard to both of these parameters. αGly147 is an "activation" hinge where backbone flexibility maintains high values for intrinsic gating, the affinity of the resting conformation for agonists and net ligand binding energy. αGly153 is a "deactivation" hinge that maintains low values for these parameters. αTrp149 (between these two glycines) serves mainly to provide ligand binding energy for gating. We propose that a concerted motion of the two glycine hinges (plus other structural elements at the binding site) positions αTrp149 so that it provides physiologically optimal binding and gating function at the nerve-muscle synapse.

Introduction

At the vertebrate neuromuscular synapse, transmitter molecules released from the nerve terminal bind at two specific sites in the extracellular domain of the nicotinic acetylcholine receptor (AChR) to promote opening of a distant ion channel and depolarization of the muscle cell membrane (Edelstein and Changeux, 1998; Karlin, 2002; Auerbach, 2010). The equilibrium constant of the AChR "gating" conformational change is coupled to an affinity change for agonists at the transmitter binding sites. Acetylcholine (ACh) binds more tightly to active-open (R*) compared with resting-closed (R) AChRs, hence there is a higher probability that liganded receptors will adopt the R*, open-channel conformation compared with unliganded receptors. Each AChR transmitter binding site is composed, in part, of three loops in the α subunit. Here we are concerned with the roles of residues in loop B with regard to the agonist affinity change and the global gating isomerization.

The probability of adopting R* is reduced by mutations of aromatic residues at the binding sites (Dennis et al., 1988; Abramson et al., 1989; Galzi et al., 1990; Cohen et al., 1991; Middleton and Cohen, 1991; Aylwin and White, 1994;

O'Leary et al., 1994; Sine et al., 1994; Chen et al., 1995; Chiara et al., 1998; Akk, 2001). Phe mutations of αTrp149 (loop B) and αTyr190 (loop C) decrease the affinity of the R conformation for ACh but, to an even greater extent, that of the R* conformation (Purohit and Auerbach, 2010). Residues αTyr93 (loop A), αTyr198 (loop C), and ε/δ subunit position Trp55/Trp57 (loop D) show similar, but less pronounced, behaviors. Most of these mutations have relatively smaller effects on the unliganded gating equilibrium constant (E_0), so the primary mechanism by which they decrease activation of fully liganded AChRs is by decreasing the net ligand binding energy available for gating. This energy is proportional to the natural logarithm of the R/R* equilibrium dissociation constant ratio (λ, the "coupling" constant). Loop B contains two glycines at positions αGly147 and αGly153 and a conserved Trp at position αTrp149. Our goal was to estimate the effects of mutations of these and other loop B amino acids with regard to both E_0 and λ.

Some loop B residues have been studied previously. αG153S is a slow channel congenital myasthenic mutation (Sine et al., 1995) that yields AChRs with a higher R-conformation affinity for the transmitter and an increased intrinsic gating isomerization constant (Zhou et al., 1999). This residue has recently been suggested to be important with regard to setting the AChR affinity specifically for the partial agonist nicotine (Xiu et al., 2009). αTrp149 has long been known to play a central role in both agonist binding and channel gating (Zhong et al., 1998; Akk, 2001). Many mutations here increase E_0 (Purohit and Auerbach, 2010), but, because they

---

ABBREVIATIONS: AChR, nicotinic acetylcholine receptor; ACh, acetylcholine; R, resting-closed AChRs; R*, active-open state AChRs; PBS, phosphate-buffered saline; wt, wild type; P_o, open probability; R/E, rate-equilibrium; Cho, choline.

also substantially reduce the R affinity, their effects on liganded gating have not yet been quantified. Less is known about the contributions of other loop B residues in ligand binding and channel gating. αThr148 and αThr150 mutations have little effect on agonist binding or channel gating (Lee and Sine, 2004; Cashin et al., 2007), αTyr151 is required for strong binding of imidacloprid to insect AChRs (Liu et al., 2005), and αAsp152 is important for setting both the affinity of the resting binding site and the diliganded gating equilibrium constant (Sugiyama et al., 1996; Zhou, 1999). In sum, pieces of information about ligand binding and channel gating are known for loop B residues, but a full exposition of the effects of mutations here is currently not available.

We have carried out a systematic single-channel study of α subunit loop B residues αGly147–αGly153. For each position, we dissect the underlying cause of its influence on AChR function with regard to E_0 and λ.

Materials and Methods

Mutagenesis and Expression. Mutants were made by using the QuikChange site-directed mutagenesis kit (Stratagene, La Jolla, CA) and were confirmed by complete cDNA sequencing. Human embryonic kidney 293 cells were transiently transfected using calcium-phosphate precipitation with a mixture of cDNAs encoding mouse muscle AChRs (α, β, δ, and ε; ~3–4 μg/35 mm dish, in the ratio 2:1:1:1). cDNA (0.1 μg/μl) encoding green fluorescent protein was added as a marker to the transfection cocktail. The cells were incubated at 37°C, the culture medium was washed after ~16 h, and single-channel patch clamp recording was performed in the cell-attached configuration ~4 to 6 h later at 23°C. The bath solution was usually Dulbecco's phosphate-buffered saline (PBS) containing 137 mM NaCl, 0.9 mM CaCl$_2$, 2.7 mM KCl, 1.5 mM KH$_2$PO$_4$, 0.5 mM MgCl$_2$, and 8.1 mM Na$_2$HPO$_4$, pH 7.4. Sometimes, NaCl was replaced with KCl (K-PBS) in the bath solution. The pipette solution was always PBS. In some experiments, an agonist (acetylcholine or choline) was added only to the pipette solution. The pipette potential was either +70 (PBS) or −70 mV (K-PBS), which corresponds to membrane potentials of approximately −100 or exactly +70 mV. Currents were sampled at 50 kHz after low-pass filtering at 20 kHz. QuB software (http://www.qub.buffalo.edu) was used to acquire and analyze the single-channel currents.

The single-channel currents were corrected for baseline drift. Clusters of single-channel openings, which each reflect binding and gating events of an individual AChR, were selected by eye and idealized into noise-free conducting/nonconducting intervals by using the segmental-k_means algorithm (Qin, 2004). To estimate the gating rate constants, the idealized current interval durations were modeled using a maximum interval likelihood method after imposing a 25-μs dead time and approximate missed-event correction (Qin et al., 1997).

The scheme we used for interpreting the functional properties of AChRs is shown in Fig. 1B. The diliganded gating equilibrium constant (E_2) was calculated as the ratio of the forward/backward isomerization rate constants (f_2/b_2). Choline was used to activate constructs in which E_2 was approximately equal to or larger than that of the wild type (wt), and ACh was used to activate constructs in which E_2 was smaller than that of the wt. In most experiments, the initial test agonist concentration was either 20 mM choline or 1 mM ACh.

Some loop B mutations caused a severe loss of activity so that openings were not clustered even at these high agonist concentrations. To compensate, we coexpressed these mutants with an ε subunit having two transmembrane domain background mutations, ε(P245L+L269F). Together, these two mutations increase f_2 by ~14-fold and decrease b_2 by ~33-fold (increase E_2 by ~450-fold). The

background mutations were located far from loop B, ao we assumed that their effects and those at loop B were energetically independent.

In some experiments, we fully saturated the transmitter binding sites by using 140 mM acetylcholine, a concentration that is ~1000 times larger than the resting equilibrium dissociation constant (K_d) of wt AChRs (Chakrapani et al., 2003). To be sure that this concentration fully saturated the binding sites, we also measured the gating rate constants at 100 mM ACh. If the effective opening rate was approximately the same at both concentrations, we considered the binding sites to be completely saturated (Supplemental Fig. S2).

At these high ACh concentrations, open-channel block by the agonist reduced the current amplitude almost to zero. To compensate, in some experiments, the pipette was held at −70 mV (which corresponds to a membrane potential of +70 mV) and the kinetic parameters of the outward, single-channel currents were quantified. Depolarization also changes the gating rate constants. Because we wanted to compare the measured equilibrium and rate constants with wt values obtained at a physiological membrane voltage (~−100 mV) we used correction factors that pertain to a 170-mV depolarization, which alone causes a 1.5-fold decrease in f_2 and 10-fold increase in b_2 (a 15-fold decrease in E_2) (Auerbach et al., 1996; Jha et al., 2009). We assumed that the voltage and mutation perturbations are energetically independent. The background perturbation corrected constants are reported in Supplemental Table S1. All experiments with 20 mM choline were at −100 mV membrane potential. To correct for the effect of channel-block on b_2, we multiplied the observed value by 3.1 (corrected values shown in Supplemental Table S1) (Jha et al., 2009).

K_d was estimated for some mutants (Fig. 3, Supplemental Table S4). For the αGly153 series, AChRs were activated by using three different choline concentrations, and interval durations within clusters were fitted together by using the kinetic scheme R$\leftrightarrow$ RA$\leftrightarrow$ A$_2$R$\leftrightarrow$ A$_2$ R*, where A is the agonist. We assumed that the two binding steps are equal and independent (Akk et al., 1996; Salamone et al., 1999; Jha et al., 2009), so only four rate constants were free parameters: single-site association (k_+) scaled by the agonist concentration, single-site dissociation (k_-), f_2 and b_2. K_d was calculated as the ratio k_-/k_+. For αG147S the relationship between the [ACh] and the open probability of clusters (P_o) was fitted by (from the scheme above): $P_o = (c^2E_2)/(1 + 2c + c^2 + c^2E_2)$; $c = $ [ACh]/K_d. At each ACh concentration, P_o was calculated from the rate constants: $P_o = f_2/(f_2+b_2)$.

In wt AChRs, unliganded (spontaneous) openings are both rare and brief. To increase both the frequency and duration of such openings, we used a background construct that had multiple point mutations in both α subunits (αD97A+αY127F+αS269I; 'DYS'). Individually, each of these mutations increases the diliganded gating equilibrium constant [αD97A, 168-fold (Chakrapani et al., 2003); αY127F, 59-fold (Purohit and Auerbach, 2007); and αS269I, 115-fold (Mitra et al., 2005)] by an approximately parallel change in the unliganded gating equilibrium constant (Purohit and Auerbach, 2009). None of these mutations has a significant effect on K_d. The fold changes in E_0 for the loop B mutations in this study are expressed in reference to the DYS background, so the only assumption we make is that the loop B and DYS mutations have independent energetic consequences. There was no agonist-associated open-channel block in experiments without agonists in the pipette solution, and the single-channel current amplitude was in all cases ~7 pA at a pipette potential of +70 mV.

For some mutants, the spontaneous open- and closed-interval durations within clusters were well described by a single exponential component. For these, f_0 and b_0 were simply the inverse mean lifetimes of the nonconducting and conducting intervals. In some constructs there were multiple open/shut components, and for these the intracluster interval durations were fitted by using a kinetic model having two nonconducting and two conducting states. We tested both coupled and uncoupled kinetic schemes, with nearly equivalent results for the E_0 estimate. The values reported in the
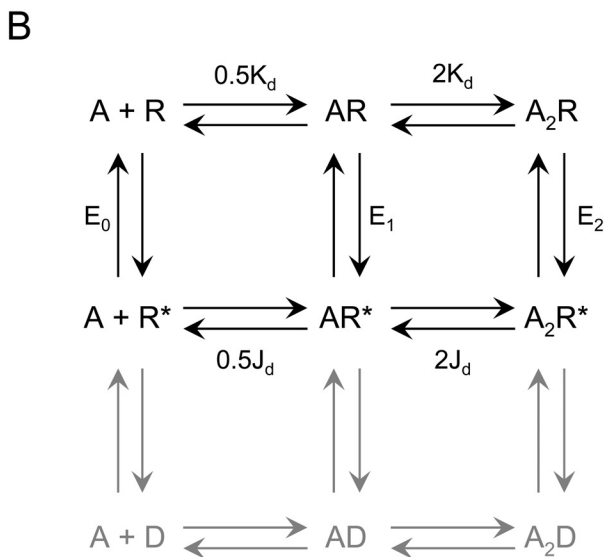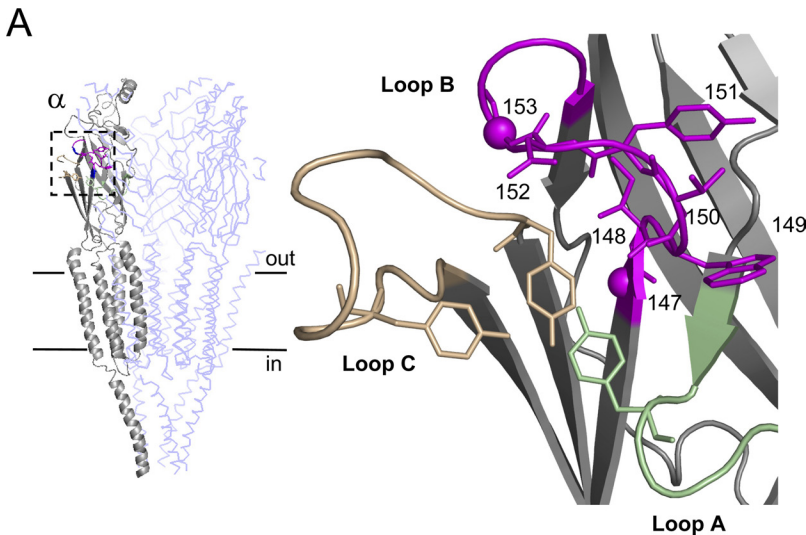
Tables were obtained by using a coupled conducting-state model (CCOO), with E_0 calculated as the ratio of f_0/b_0 associated with the predominant (typically, ~90%), brief open component.

For each mutant, the fold change in parameter X was estimated as ($X^{mutant}/X^{background}$). The change in the free energy ($\Delta\Delta G$, in kilocalories per mole) caused by mutation was calculated as $-0.59\ln$(fold change). The coupling energy between side chains was calculated as $-0.59\ln(X^{observed}/X^{predicted})$, where the predicted value was calculated as the sum of the $\Delta\Delta G$ values for each individual mutation.

For all constructs, example currents are shown in Supplemental Fig. S1, and the rate constants are shown in Supplemental Tables S1 and S2. The kinetic parameters are displayed in the form of rate-equilibrium (R/E) relationships, in which the forward isomerization rate constant is plotted as a function of the gating equilibrium constant for a family of mutations of that residue on a log-log scale (Fersht, 1995). The "range-energy" is the natural logarithm of the ratio of the largest/smallest equilibrium constant for a series of mutations of one position (Jha et al., 2009). Φ is the linear slope of the R/E relationship and provides information about the relative timing of the energy change of the perturbed residue, on a scale from 1 (early) to 0 (late).

Results

An unliganded *Torpedo californica* AChR transmitter binding site is shown in Fig. 1, A and B (Unwin, 2005). The model we used for quantifying AChR function is a cyclic activation scheme (Fig. 1C). In this scheme the resting R state has a low affinity for ACh and a closed channel, and the active R* state has a high affinity for ACh and an open channel. The R and R* shapes must be different insofar as they have different functional properties.

The cyclic scheme predicts that AChRs should open and close spontaneously, in the absence of exogenous agonists (the R↔ R* step). Such events are indeed present in wt AChRs. Jackson (1986)) estimated that in embryonic mouse muscle, the unliganded gating equilibrium constant $E_0 \sim 10^{-7}$. In adult mouse muscle AChRs expressed in human embryonic kidney cells, $E_0 \sim 6.5 \times 10^{-7}$ (Purohit and Auerbach, 2009; Jha and Auerbach, 2010). In AChRs the allosteric constant E_0 is small, but it is measurably different from zero. Mutations that increase E_0 in human AChRs are the fundamental cause of some congenital myasthenic syndromes (Zhou et al., 1999).

The adult mouse AChR binding sites have approximately equal affinities for ACh (Salamone et al., 1999; Jha and Auerbach, 2010), so there are only four equilibrium constants to consider in the cyclic scheme: the dissociation constant of the R conformation (K_d), the dissociation constant of the R*

Fig. 1. AChR structure and function. A, the transmitter binding site. Left, unliganded *T. californica* AChR [Protein Data Bank code 2BG9 (Unwin, 2005)]. Subunits: α_g, gray; β/δ, light blue (γ and α_d not displayed). Boxed area is the α_g transmitter binding site. Horizontal lines approximate the location of the membrane. Right, close-up of the α_g binding site. Green, loop A (αTyr93 shown); tan, loop C (αTyr190 shown); magenta, loop B (all side chains 147–153 shown, Cα atoms of αGly147 and αGly153 as spheres). B, cyclic activation scheme for the AChR. A is the agonist and the other bold letters represent stable ground states (structural ensembles represented by wells in an energy diagram). Paired arrows represent the unstable intermediates that connect the ground states. R, resting (low affinity for the agonist and low ionic conductance); R*, active (high affinity for the agonist and high ionic conductance); D, desensitized states (high affinity for the agonist and low ionic conductance) are gray. Next to the arrows are the salient equilibrium constants. E_0, unliganded (spontaneous) gating; E_1, monoliganded gating; E_2 diliganded gating; K_d, dissociation constant for agonist binding to R; J_d, dissociation constant for agonist binding to R*. The two binding sites have approximately the same K_d and J_d for ACh and choline (Jha and Auerbach, 2010). Without an external energy source, the net energy change, R to A$_2$R*, must be equal for the "physiological" pathway R↔ AR↔ A$_2$R↔ A$_2$R* and for the alternative pathway R↔ R*↔ AR*↔ A$_2$R*. Hence, $E_2/K_d^2 = E_0/J_d^2$, or $E_2 = E_0\lambda^2$.

conformation (J_d), the diliganded gating constant (E_2), and the allosteric constant (E_0). Without an external energy source, the energy required to move from R to A_2R^* must be the same for the clockwise and counterclockwise paths, hence $E_2 = E_0\lambda^2$, where $\lambda = K_d/J_d$. The efficacy of an agonist (which is a function only of E_2) is the product of two more-fundamental parameters: the allosteric constant (E_0) and the coupling constant (λ) at two transmitter binding sites. In our wt preparation, $\lambda^{ACh} \approx 6600$.

Our objective was to measure E_2 and E_0 for different loop B mutations and calculate λ [$\sqrt{(E_2/E_0)}$]. For each mutation, the energy (kilocalories per mole) from the ligand affinity change is $\Delta G^{bind} = -0.59\ln(\lambda)$, and the energy change for unliganded gating is $\Delta\Delta G^{gate} = -0.59\ln(E_0^{mut}/E_0^{wt})$. In wt AChRs, we estimate that each ACh molecule is $\Delta G^{bind} = \sim -5.2$ kcal/mol more stably bound in R* versus R. We also calculated the change in binding energy caused by the mutation, $\Delta\Delta G^{bind} = \Delta G^{bind, mut} - \Delta G^{bind, wt}$.

αGly147. The results for αGly147 are summarized in Fig. 2. This residue is conserved in mouse AChR α-subunits and is also present in the acetylcholine binding protein. We examined 10 different side chain substitutions of this amino acid (Ala, Ser, Val, Asp, Glu, Arg, Lys, Trp, Tyr, and Pro), but single-channel currents activated by 1 mM ACh were apparent only with the Ser, Ala, and Val mutants. Some of the silent αGly147 mutations express functional AChRs. The αG147S, Ala and Val single-channel currents were apparent but did not occur in clusters when activated by 1 mM ACh. The effective opening rate at this concentration (R→A_2R^*) is small because either K_d was large, E_2 was small, or both.

To enhance cluster formation and allow the estimation of gating rate and equilibrium constants, we expressed these mutants on a background that increased E_2 by ~450-fold (see Supplemental Fig. S1 for example current traces). This background "boosts" E_0 to allow cluster formation and rate constant estimation but has no effect on the loop B mutation's effects on E_0 or λ. Using this background, and by fully saturating the transmitter binding sites by using 140 mM ACh (Supplemental Fig. S2), we estimate that the αG147S, Ala and Val mutations indeed decrease E_2^{ACh} substantially (Supplemental Table S1).

Our next objective was to measure E_0 for the αGly147 mutants. For these experiments, we used a background construct that was active spontaneously so that the effect of the loop B mutation could be estimated directly from the durations of intervals within spontaneous clusters (Purohit and Auerbach, 2009). With this background, 6 of the 10 substitutions at αGly147 (Ala, Ser, Val, Glu, Lys, Tyr) produced spontaneous single-channel current clusters. Asp, Arg, Pro, and Trp side-chain substitutions did not result in the expression of functional AChRs. All of the expressing mutants reduced E_0 relative to the background (Supplemental Table
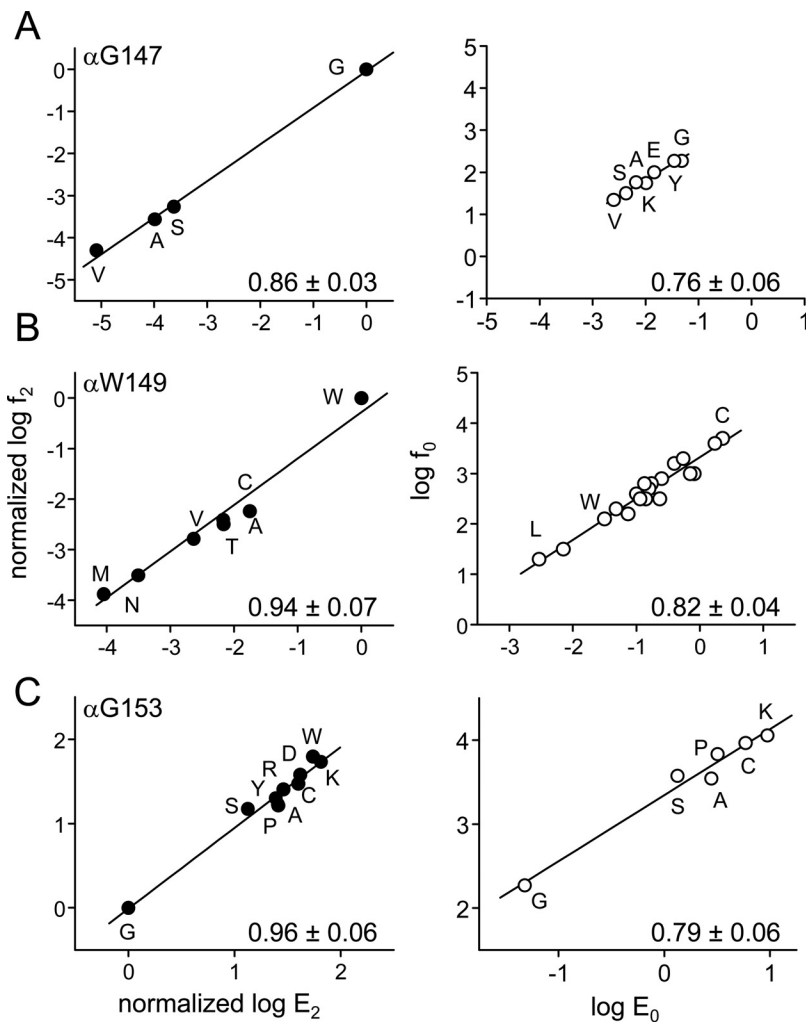

Fig. 2. R/E relationships for three loop B residues. Left, diliganded gating; right, unliganded (spontaneous) gating. The x-axis is the logarithm of the gating equilibrium constant (E_2 or E_0) and the y-axis is the logarithm of the forward, channel-opening rate constant (f_2 or f_0). A, αGly147 mutations reduce E_2 more so than E_0. B, αTrp149 mutations reduce E_2 but mainly increase E_0 [values from Purohit and Auerbach (2010)]. C, αGly153 mutations increase E_2 and E_0 to similar extents (Fig. S3). The kinetic parameters are shown in Supplemental Tables S1 and S2. The number in each panel is the R/E slope (Φ) ± S.D. of the linear fit, which gives the relative timing of the residue's gating motion (larger is earlier). All three residues move early, but the diliganded Φ values are larger than the unliganded ones.

S2). However, even the largest reduction (αG147V) was modest, only ~20-fold less than the background.

With these estimates of E_0 and E_2 for the Ser, Ala, and Val mutants of αGly147, we calculated λ and ΔG^{bind} for ACh (Supplemental Table S3). On average, for these three αGly147 mutants λ^{ACh} ~ 194 and $\Delta\Delta G^{bind}$ ~ +2.1 kcal/mol. Compared with the wt values for ACh, these mutations decreased the net ACh binding energy by ~60%. In contrast, the average effect of these mutations on the allosteric constant was smaller ($\Delta\Delta G^{gate}$ ~ +1.4 kcal/mol). The main effect of mutating αGly147 is to reduce the amount of energy made available by the affinity change at the transmitter binding site.

The slope of the R/E plot (Φ) for the αGly147 diliganded gating was 0.86 (Fig. 2A). This indicates that with ACh present in the binding sites, this residue experiences a change in energy near the onset of the channel-opening process, at approximately the same time as the energy change of the agonist molecule itself (Grosman et al., 2000). Interestingly, the Φ value for the unliganded reaction (0.76), although high, was smaller than that for the diliganded reaction.

The reduction in λ^{ACh} in αG147S could be caused by an increase in the R affinity (a decrease in K_d), a decrease in the R* affinity (an increase in J_d), or both. We estimated K_d by examining the αG147S mutant activated by different concentrations of ACh (Fig. 3A). We estimate that K_d for ACh in this construct is ~3.6 mM, which is ~25 times higher than that of the wt (Chakrapani et al., 2003). Using the E_2 and E_0 values for this mutant and the equation $E_2 = E_0\lambda^2$, we calculate that J_d for ACh in this construct is 12.1 μM, which is ~550 times higher than that of the wt (Jha and Auerbach, 2010). Thus, the reduction in the amount of energy made available by the affinity change at the transmitter binding site can be attributed mainly to a decreased affinity for ACh in the R* conformation of the binding site.

α**Trp149.** αTrp149 is an important binding site residue that provides binding energy to the ligand in both the R and R* conformations, probably by cation-π interactions (Zhong et al., 1998). We have shown previously that mutations of αTrp149 also influence E_0 (Purohit and Auerbach, 2010). Some of these mutations caused a substantial increase in E_0 ($\Delta\Delta G^{gate}$ = −2.3 kcal/mol for αW149C), but most had more modest or negligible effects ($\Delta\Delta G^{gate}$ = +0.3 kcal/mol for αW149M).

We measured the effects of αTrp149 mutations on diliganded gating to estimate λ^{ACh} (Fig. 2B and Supplemental Fig. 1S). All of the tested mutations reduced E_2, the largest effect being a ~10,000-fold reduction for αW149M (Supplemental Table S1). For all mutants, the predominant effect was to reduce the net agonist binding energy. The clearest example is αW149M, for which E_0 was almost unchanged but λ^{ACh} decreased by ~80-fold ($\Delta\Delta G^{bind}$ = +2.6 kcal/mol). On average, the αTrp149 mutations reduced the R versus R* ACh binding energy by ~50%. As was the case with αGly147, the diliganded Φ value for αTrp149 was higher than the corresponding value for unliganded gating (0.94 versus 0.82) (Fig. 2B).

α**Gly153.** αGly153 is an interesting loop B residue, because a Ser here reduces K_d and causes a myasthenic syndrome (Sine et al., 1995). In addition, AChRs that have a high affinity for nicotine (with $\alpha2$, $\alpha3$, or $\alpha4$ subunits) have Lys here, whereas those that do not ($\alpha1$ or $\alpha7$) have a Gly. We measured E_0 and E_2 for several αGly153 mutants. In these experiments, we used the partial agonist choline (Cho) because αGly153 mutations increased the opening rate constant to such an extent that it was not possible to obtain estimates using ACh.
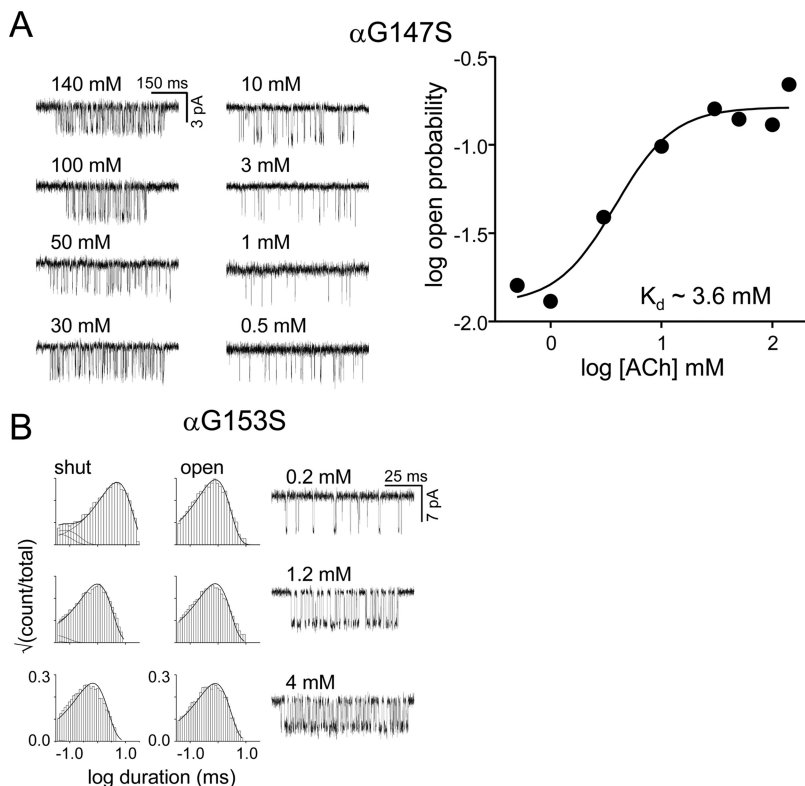

Fig. 3. Equilibrium dissociation constants. A, the affinity of the resting αG147S AChR for ACh was estimated from the P_o dose-response profile. B, K_d values for choline were estimated for αG153S by fitting interval durations across concentrations. The rate constants and K_d values for all αGly153 mutants were similar and are given in Supplemental Table S4.

All of the tested αGly153 side-chain substitutions (Lys, Trp, Asp, Cys, Arg, Tyr, Ala, Pro, and Ser) produced functional AChRs that had a higher E_2 values compared with wt (Fig. 2C and Supplemental Table S1). We also measured E_0 for all nine of these αGly153 mutants. AChRs with Trp, Asp, Arg, or Tyr substitutions produced single-channel currents having multiple open/closed components. The fractional contribution of each of these components was variable between patches, to an extent that E_0 could not be estimated reliably. The other substitutions had more simple kinetic behavior and exhibited clearly predominant open and closed components. All of these substitutions increased E_0 relative to the background, from 206-fold for Lys to 28-fold for Ser (Supplemental Table S2).

The fold-changes in E_2 versus E_0 for the αGly153 mutations are shown in Supplemental Fig. S3. The maximum effect on both E_2 and E_0 was for the Lys substitution. Overall, the fold changes in E_2 and E_0 were linearly correlated ($r^2 = 0.99$) (Supplemental Fig. S3). This result indicates that αGly153 mutations alter diliganded gating by an approximately parallel change E_0 and have almost no effect on λ^{Cho} (Supplemental Table S3). Indeed, the average $\Delta\Delta G^{\mathrm{bind}}$ for the Lys, Cys Ala, Pro, and Ser mutants was only +0.3 kcal/mol. Although αGly153 mutations increase the affinity of the resting binding site, they have the same quantitative effect on the affinity of the active binding site. We conclude that αGly153 makes essentially no contribution to the binding energy difference between R and R*. As was the case for αGly147 and αTrp149, the αGly153 diliganded Φ-value was higher than that for unliganded gating (0.96 versus 0.79) (Fig. 2C).

We also measured the single-site association and dissociation rate constants and equilibrium dissociation constant for Cho binding to the resting conformation for four different αGly153 mutants (Ser, Ala, Asp, and Lys) (Fig. 3B and Supplemental Table S4). All of the mutations reduced K_d (increased the resting affinity) compared with the wt (Supplemental Table S4) to approximately the same extent (mean, ~14-fold).

Other Loop B Mutations. We measured E_2 and E_0 for Ala side-chain substitutions at the five residues between the two loop B glycines (Thr148, Trp149, Thr150, Tyr151, and Asp152). All of these constructs except αW149A resulted in only small (<2-fold) changes in both E_2 and E_0 compared with the wt (Tables S1 and S2 and Supplemental Fig. S1F). In αW149A, E_0 increased by ~8-fold, but E_2 decreased by ~134-fold. Using the equation $E_2 = E_0\lambda^2$, we estimate that for this mutant, $\lambda^{\mathrm{ACh}} \sim 200$ and $\Delta\Delta G^{\mathrm{bind}} = +2.0$ kcal/mol.

The E_0 values were estimated for a few additional mutants of these positions (Supplemental Table S2 and Supplemental Fig. S1). At residue αAsp152, only the Ala substitution resulted in functional AChRs (no currents for Trp, Lys, Arg, or Tyr). At positions αThr148, αThr150, and αTyr151, the largest fold decrease in E_0 was for αT150Y (~25-fold).

Global estimates for the energetic consequences of loop B perturbations from R/E plots for all the mutants are shown in Supplemental Fig. S4. The Φ-values for diliganded and unliganded gating were 0.92 and 0.77, respectively. The largest fold increase in E_0 was for αG153K and the largest fold decrease was for αT150Y. This range (for both α-subunits combined) corresponds to an energy of ~5.5 kcal/mol.

Multiple Open-Channel Lifetimes. We now turn to the description of multiple open-time components, which are common in unliganded AChRs (Jackson, 1986; Grosman, 2003; Mukhtasimova et al., 2009; Purohit and Auerbach, 2009). These events are worth examining, in part, because they have been interpreted as reflecting an intermediate state in the channel-opening conformational cascade (Mukhtasimova et al., 2009). We reported previously that many binding site mutations eliminate this long-lived component [αTyr93 (loop A), αTrp149 (loop B), and αTyr190/αTyr198 (loop C)], even when combined with distant mutations in the transmembrane domain that alone make it more prevalent simply because these have low Φ values and therefore slow all closures (Purohit and Auerbach, 2010). This observation led us to conclude that the long openings arise from local structural fluctuations of binding site residues, primarily of αTrp149.

αGly153 mutations did not eliminate the long-open component and, in fact, enhanced them in some cases. We therefore tested whether or not substitutions at the abovementioned positions that eliminate spontaneous long openings do so when a αG153S mutation is also present (Fig. 4). We examined five double-mutant pairs, αG153S+[αW149F, αY93F, αY190F, αY198F, or αG147S] where the bracketed mutation was previously shown to eliminate long openings. The αW149F, αY198F, and αG147S mutations again eliminated the long-open component, but the αY93F and αY190F substitutions no longer did.

Inter-residue coupling energies for αG153S paired with a Phe substitution at four α subunit binding site aromatic residues (αTyr93, αTrp149, αTyr190, and αTyr198) and αGly147 are shown in Supplemental Table S5. In all cases, the Ser-Phe side-chain pairs behaved nearly independently in unliganded gating.

Discussion

The results (summarized in Fig. 5 and Table 1) provide insight into the nature of the energy changes at the AChR transmitter binding site when it changes conformation be-
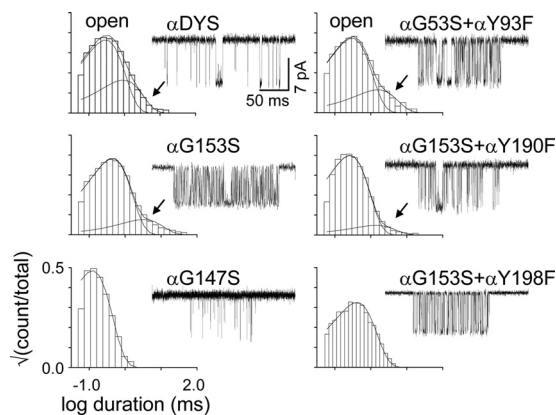

Fig. 4. Multiple open components. Example histograms and single-channel current traces for different loop B mutants. Arrow indicates the long-opening component. There was no agonist present (spontaneous currents). In all constructs, the background was αDYS (Supplemental Data). Long openings are apparent in the background (no binding site mutations) and with the binding site mutations αG153S, (αG153S+αY93F), and (αG153S+αY190F). They were absent with the mutations (αG153S+αG147S) and (αG153S+αY198F). The long openings possibly arise from a local isomerization of αTrp149 (Purohit and Auerbach, 2010).

tween its low-affinity R and high-affinity R* conformation. It is this change in conformation that triggers the gating conformational cascade and determines ligand efficacy.

In brief, αGly147 and αGly153 seem to act as hinges that influence the allosteric constant (E_0), the resting affinity (K_d), and the agonist affinity ratio (λ). However, these hinges have opposite actions. Mutations of αGly147 change the above parameters so that there is a decrease in P_o, whereas αGly153 mutations change them to cause an increase in P_o. Below, we associate a change in energy with a local change in structure (a "strain" or "movement" of the perturbed position
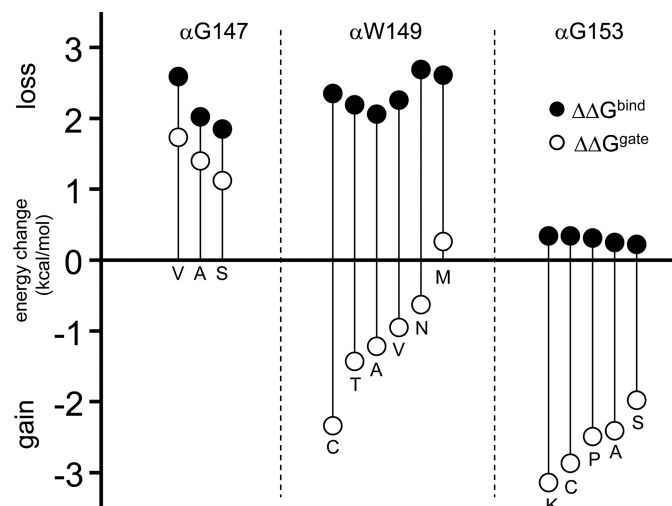

Fig. 5. Binding site mutations change the energy of intrinsic gating and agonist binding. Closed symbols, the gating free energy change [$\Delta\Delta G^{gate} = -0.59\ln(E_0^{mut}/E_0^{wt})$, in kilocalories/mole]. Open symbols, the binding free energy change or [$\Delta\Delta G^{bind} = -0.59\ln(\lambda^{mut}/\lambda^{wt})$]. Favorable mutations (that produce a negative $\Delta\Delta G$) increase the P_o. Left, αGly147 mutations are unfavorable with regard to both gating and binding, but the effect is larger for binding. Center, αTrp149 mutations mostly are favorable with regard to gating but have larger and unfavorable effects on binding. Right, αGly153 mutations have a large and favorable effect on gating but little effect on binding. The values are listed in Table 1.

TABLE 1

Energy changes of unliganded gating (E_0) and agonist binding (λ) for different loop B mutants

The units are kilocalories per mole. The values are shown in graphical form for αGly147, αTrp149, and αGly153 in Fig. 5. λ is the R/R* affinity ratio (K_d/J_d) for the appropriate agonist. $\Delta\Delta G^{bind} = -0.59\ln(\lambda^{mut}/\lambda^{wt})$ and $\Delta\Delta G^{gate} = -0.59\ln(E_0^{mut}/E_0^{wt})$. See Supplemental Tables S1 to S3.

Construct	Ligand	λ (K_d/J_d Ratio)	Net Binding ($\Delta\Delta G^{bind}$)	Gating ($\Delta\Delta G^{gate}$)
wt^{ACh}	ACh	6587	0.00	0.00
wt^{cho}	Cho	266	0.00	0.00
G147V	ACh	82	2.59	1.73
G147A	ACh	215	2.02	1.40
G147S	ACh	287	1.85	1.12
W149C	ACh	123	2.35	−2.34
W149T	ACh	161	2.19	−1.43
W149A	ACh	202	2.06	−1.22
W149V	ACh	143	2.26	−0.95
W149N	ACh	69	2.69	−0.63
W149M	ACh	79	2.61	0.26
G153K	Cho	151	0.34	−3.14
G153C	Cho	151	0.34	−2.87
G153P	Cho	159	0.31	−2.49
G153A	Cho	175	0.25	−2.41
G153S	Cho	184	0.22	−1.98
T148A	Cho	196	0.18	−0.28
T150A	Cho	161	0.00	−0.64
Y151A	Cho	521	−0.39	1.04
D152A	Cho	339	−0.14	0.13

relative to its immediate environment), and use the word "favorable" to describe a molecular motion that increases P_o.

αGly147 mutations reduced E_0, which is to say that in the absence of agonists, the energy change associated with the gating motion of this residue is unfavorable for all side-chain substitutions. Although we cannot with certainty identify the structural correlate(s) of this unfavorable energy change, there are some clues. Because all tested side chains substitutions were unfavorable, we speculate that in the absence of ligands, there is a favorable gating motion in the wt that requires flexibility of the backbone (an "activation" hinge). However, different amino acid substitutions caused modestly different degrees of energy change, so side-chain interactions, too, are likely to be involved. Because the larger Val side chain experienced the largest gating energy change, it is possible that steric hindrance is a factor that sets the magnitude of E_0.

Using the cyclic activation scheme and the equation $E_2 = E_0\lambda^2$ (see below), we conclude that the αG147S, -A, and -V mutants reduce λ^{ACh} from ~6600 in the wt to ~194. This corresponds to a net loss in ACh binding energy of $\Delta\Delta G^{bind} \sim$ +2.1 kcal/mol per site. The αG147S mutation reduced the affinity of both the resting and active binding sites, but the effect was larger for R* compared with R. Hence, the main effect of this mutation seems to be to reduce the stability of the bound transmitter in the R* conformation. This implies that with ligand present in wt AChRs, at the onset of the forward isomerization the structural change at αGly147 results in a net favorable energetic interaction of the protein with the transmitter molecule.

There are some hints regarding the structural basis of this event. Ser and Ala are both small and have a similar effect on λ^{ACh}, whereas the larger Val side chain had a somewhat larger effect. This suggests that $\Delta\Delta G^{bind}$ is influenced by side-chain size as well as by the elimination of the abovementioned intrinsic favorable backbone motion. αGly147 is far from the ligand (Celie et al., 2004), so this binding energy change is likely to be indirect and involve additional structural elements at the binding site. Regardless, without the activation hinge at position αGly147 the residual net ACh binding energy is reduced from −5.2 to −3.1 kcal/mol/site. Interfering with the gating motion of αGly147 decreases the binding energy used to promote gating by ~60%.

Mutations of αTrp149 had approximately the same magnitude of effect on E_0 as those at position αGly147; in contrast, without agonists, most αTrp149 side-chain substitutions were *more* stable in R* compared with R. The order of effect (C > T > A > V > N > M) does not immediately suggest a chemical basis of the more-favorable R* environment around αTrp149 in the unliganded site, except to note that the energy changes varied substantially with different side chains and that steric hindrance does not seem to be a factor. We speculate that the gating motion of αTrp149 in the unliganded binding site involves a change in the positions of side-chain atoms in a spatially unrestricted environment.

The αTrp149 mutant binding energy changes were large and unfavorable for all substitutions. There was only a small range or energies for the binding energy loss (~0.6 kcal/mol, Ala to Asn), which suggests that for the residues we examined, only Trp provides the extra stabilization energy to the bound ligand, probably via a cation-π interaction (Zhong et al., 1998). This energy constitutes approximately half of the

total net ACh binding energy change. We speculate that the residual binding energy (~-2.7 kcal/mol per site) comes from interactions between the ligand and other binding site entities, particularly αTyr190 (Purohit and Auerbach, 2010).

αGly153 is quite different from both αGly147 and αTrp149. Essentially all of the energetic effects of mutations here were with regard to E_0, with very little with regard to λ^{Cho}. In the unliganded binding site, αGly153 moves and, as was the case with αTrp149, with side-chain substitutions here, the AChR was in all cases *more* stable in R* compared with R. The fact that the E_0 range of gating energy change here was small (~1 kcal/mol) suggests that side-chain size does not play a significant role. We speculate that in both the presence and absence of agonists this glycine adopts an unfavorable R* backbone configuration (a "deactivation" hinge) and that all mutations here prevent this from happening.

Although all αGly153 mutations reduced K_d (see below), they also reduced J_d to approximately the same extent (Supplemental Table S4). We conclude that the αGly153 does not provide agonist binding energy for the gating isomerization, either directly or indirectly. This conclusion bears directly on the recent report proposing that the αGly153 side chain is the basis for differences in the EC_{50} value for the partial agonist nicotine in different AChRs (Xiu et al., 2009). The observations that led to this hypothesis were that the αG153K mutation decreases the neuromuscular EC_{50} for nicotine and restores the fingerprint of a cation-π interaction between αTrp149 and this agonist. EC_{50} is a complex parameter that reflects both binding and gating. Our results suggest that for αG153K, the 14-fold reduction in EC_{50} can be attributed almost completely to the 206-fold increase in E_0. Our evidence suggests that a Lys side chain at this position increases the efficacy of all agonists equally and not specifically that of nicotine.

Previously we reported that for seven different locations (all far from the binding sites), Φ values were the same for diliganded and unliganded gating (Purohit and Auerbach, 2009). Here, we found that the Φ values for αGly147, αTrp149, and αGly153 were all higher in the liganded versus unliganded condition. This implies that these residues experience their gating energy change relatively earlier when an agonist molecule is nearby. This could be because the residue itself moves earlier, the peak transition state for the overall protein isomerization occurs later, or both. Regardless, the shift in Φ is an indication of an "induced fit," whereby the agonist molecule perturbs (rearranges) the binding site so as to alter the timing, pathway, or ground states of the isomerization. The effect we have observed is small, and other results suggest that the cyclic scheme is still a valid approximation even with a perturbed binding site (i.e., that many different agonists have the same Φ value) (Grosman et al., 2000) and that the effect of αGly153 mutations can be explained simply by a change in E_0. Nonetheless, the shift in Φ values with versus without ligand suggests that the cyclic scheme and the equation $E_2 = E_0\lambda^2$ may not pertain in detail to all AChRs that have binding site perturbations.

An ancillary part of this study was to measure K_d and calculate J_d for a few mutant constructs of the two loop B Gly residues. These equilibrium constants pertain to ligand binding, and the underlying molecular movements for this separate process may or may not be distinct from those for gating. Mutations of αGly147 and αGly153 had opposite effects on

K_d. The αG147S mutation reduced the affinity of the resting binding site for ACh, whereas four different substitutions of αGly153 increased this affinity. Apparently, backbone flexibility at these positions, perhaps in combination, is important for allowing agonists to bind with the physiologically appropriate resting affinity.

The long openings in spontaneous currents appear to arise from a local isomerization of the αTrp149 side chain (Purohit and Auerbach, 2010). This fluctuation in structure is delicate because it can be eliminated by a variety of binding site perturbations, including the presence of an agonist molecule, all αTrp149 side-chain substitutions, and most substitutions of αGly147, αTyr93, αTyr190, and αTyr198 (but not of αGly153 and ε/δW55/57). We speculate that in the absence of a ligand there is a network of interactions, local to the binding site that permits αTrp149 to adopt alternative conformations. One of these is associated with the relatively rare, long openings.

In summary, loop B has two glycine hinges that have opposing actions in binding and gating of wt AChRs. Removal of the activation hinge at αGly147 decreases P_o by reducing K_d E_0, and λ. The main effect of interfering with this hinge is to reduce the affinity of the active conformation of the binding site and, hence, the amount of binding energy available to promote gating. In addition, mutation αGly147 eliminates long openings that likely arise from alternative conformations of αTrp149. The deactivation hinge at αGly153 plays an inverse role. Interfering with the operation of this hinge increases P_o by increasing both K_d and E_0 but has essentially no consequence with regard to λ. Mutations of αGly153 also increase the probability of long openings. Between these two hinges is αTrp149, a residue that provides approximately half of the binding energy toward the gating isomerization. It is possible that the two opposing glycine hinges act in concert (along with other elements at the binding site) to determine E_0 and K_d and to position the central tryptophan so that it provides the physiologically appropriate binding energy to generate the synaptic response.

Authorship Contributions

Participated in research design: Purohit.
Conducted experiments: Purohit.
Performed data analysis: Purohit.
Wrote or contributed to the writing of the manuscript: Purohit and Auerbach.

References

Abramson SN, Li Y, Culver P, and Taylor P (1989) An analog of lophotoxin reacts covalently with Tyr190 in the alpha-subunit of the nicotinic acetylcholine receptor. *J Biol Chem* **264:**12666–12672.

Akk G (2001) Aromatics at the murine nicotinic receptor agonist binding site: mutational analysis of the alphaY93 and alphaW149 residues. *J Physiol* **535:**729–740.

Akk G, Sine S, and Auerbach A (1996) Binding sites contribute unequally to the gating of mouse nicotinic αD200N acetylcholine receptors. *J Physiol* **496:**185–196.

Auerbach A (2010) The gating isomerization of neuromuscular acetylcholine receptors. *The Journal of Physiology* **588:**573–586.

Auerbach A, Sigurdson W, Chen J, and Akk G (1996) Voltage dependence of mouse acetylcholine receptor gating: different charge movements in di-, mono- and unliganded receptors. *J Physiol* **494:**155–170.

Aylwin ML and White MM (1994) Ligand-receptor interactions in the nicotinic acetylcholine receptor probed using multiple substitutions at conserved tyrosines on the alpha subunit. *FEBS Lett* **349:**99–103.

Cashin AL, Torrice MM, McMenimen KA, Lester HA, and Dougherty DA (2007) Chemical-scale studies on the role of a conserved aspartate in preorganizing the agonist binding site of the nicotinic acetylcholine receptor. *Biochemistry* **46:**630–639.

Celie PH, van Rossum-Fikkert SE, van Dijk WJ, Brejc K, Smit AB, and Sixma TK (2004) Nicotine and carbamylcholine binding to nicotinic acetylcholine receptors as studied in AChBP crystal structures. *Neuron* **41:**907–914.

Chakrapani S, Bailey TD, and Auerbach A (2003) The role of loop 5 in acetylcholine receptor channel gating. *J Gen Physiol* **122:**521–539.

Chen J, Zhang Y, Akk G, Sine S, and Auerbach A (1995) Activation kinetics of recombinant mouse nicotinic acetylcholine receptors: mutations of alpha-subunit tyrosine 190 affect both binding and gating. *Biophys J* **69:**849–859.

Chiara DC, Middleton RE, and Cohen JB (1998) Identification of tryptophan 55 as the primary site of [^{3}H]nicotine photoincorporation in the gamma-subunit of the *Torpedo* nicotinic acetylcholine receptor. *FEBS Lett* **423:**223–226.

Cohen JB, Sharp SD, and Liu WS (1991) Structure of the agonist-binding site of the nicotinic acetylcholine receptor. [^{3}H]Acetylcholine mustard identifies residues in the cation-binding subsite. *J Biol Chem* **266:**23354–23364.

Dennis M, Giraudat J, Kotzyba-Hibert F, Goeldner M, Hirth C, Chang JY, Lazure C, Chrétien M, and Changeux JP (1988) Amino acids of the *Torpedo marmorata* acetylcholine receptor alpha subunit labeled by a photoaffinity ligand for the acetylcholine binding site. *Biochemistry* **27:**2346–2357.

Edelstein SJ and Changeux JP (1998) Allosteric transitions of the acetylcholine receptor. *Adv Protein Chem* **51:**121–184.

Fersht AR (1995) Characterizing transition states in protein folding: an essential step in the puzzle. *Curr Opin Struct Biol* **5:**79–84.

Galzi JL, Revah F, Black D, Goeldner M, Hirth C, and Changeux JP (1990) Identification of a novel amino acid alpha-tyrosine 93 within the cholinergic ligands-binding sites of the acetylcholine receptor by photoaffinity labeling. Additional evidence for a three-loop model of the cholinergic ligands-binding sites. *J Biol Chem* **265:**10430–10437.

Grosman C (2003) Free-energy landscapes of ion-channel gating are malleable: changes in the number of bound ligands are accompanied by changes in the location of the transition state in acetylcholine-receptor channels. *Biochemistry* **42:**14977–14987.

Grosman C, Zhou M, and Auerbach A (2000) Mapping the conformational wave of acetylcholine receptor channel gating. *Nature* **403:**773–776.

Jackson MB (1986) Kinetics of unliganded acetylcholine receptor channel gating. *Biophys J* **49:**663–672.

Jha A and Auerbach A (2010) Acetylcholine receptor channels activated by a single agonist molecule. *Biophys J* **98:**1840–1846.

Jha A, Purohit P, and Auerbach A (2009) Energy and structure of the M2 helix in acetylcholine receptor-channel gating. *Biophys J* **96:**4075–4084.

Karlin A (2002) Emerging structure of the nicotinic acetylcholine receptors. *Nat Rev Neurosci* **3:**102–114.

Lee WY and Sine SM (2004) Invariant aspartic Acid in muscle nicotinic receptor contributes selectively to the kinetics of agonist binding. *J Gen Physiol* **124:**555–567.

Liu Z, Williamson MS, Lansdell SJ, Denholm I, Han Z, and Millar NS. (2005) A nicotinic acetylcholine receptor mutation conferring target-site resistance to imidacloprid in *Nilaparvata lugens* (brown planthopper). *Proc Natl Acad Sci USA* **102:**8420–8425.

Middleton RE and Cohen JB (1991) Mapping of the acetylcholine binding site of the nicotinic acetylcholine receptor: [^{3}H]nicotine as an agonist photoaffinity label. *Biochemistry* **30:**6987–6997.

Mitra A, Cymes GD, and Auerbach A (2005) Dynamics of the acetylcholine receptor pore at the gating transition state. *Proc Natl Acad Sci USA* **102:**15069–15074.

Mukhtasimova N, Lee WY, Wang HL, and Sine SM (2009) Detection and trapping of intermediate states priming nicotinic receptor channel opening. *Nature* **459:**451–454.

O'Leary ME, Filatov GN, and White MM (1994) Characterization of *d*-tubocurarine binding site of *Torpedo* acetylcholine receptor. *Am J Physiol* **266:**C648–C653.

Purohit P and Auerbach A (2007) Acetylcholine receptor gating: movement in the α-subunit extracellular domain. *J Gen Physiol* **130:**569–579.

Purohit P and Auerbach A (2009) Unliganded gating of acetylcholine receptor channels. *Proc Natl Acad Sci USA* **106:**115–120.

Purohit P and Auerbach A (2010) Energetics of gating at the apo-acetylcholine receptor transmitter binding site. *J Gen Physiol* **135:**321–331.

Qin F (2004) Restoration of single-channel currents using the segmental k_{-}means method based on hidden Markov modeling. *Biophys J* **86:**1488–1501.

Qin F, Auerbach A, and Sachs F (1997) Maximum likelihood estimation of aggregated Markov processes. *Proc Biol Sci* **264:**375–383.

Salamone FN, Zhou M, and Auerbach A (1999) A re-examination of adult mouse nicotinic acetylcholine receptor channel activation kinetics. *J Physiol* **516:**315–330.

Sine SM, Ohno K, Bouzat C, Auerbach A, Milone M, Pruitt JN, and Engel AG (1995) Mutation of the acetylcholine receptor alpha subunit causes a slow-channel myasthenic syndrome by enhancing agonist binding affinity. *Neuron* **15:**229–239.

Sine SM, Quiram P, Papanikolaou F, Kreienkamp HJ, and Taylor P (1994) Conserved tyrosines in the alpha subunit of the nicotinic acetylcholine receptor stabilize quaternary ammonium groups of agonists and curariform antagonists. *J Biol Chem* **269:**8808–8816.

Sugiyama N, Boyd AE, and Taylor P (1996) Anionic residue in the alpha-subunit of the nicotinic acetylcholine receptor contributing to subunit assembly and ligand binding. *J Biol Chem* **271:**26575–26581.

Unwin N (2005) Refined structure of the nicotinic acetylcholine receptor at 4 Å resolution. *J Mol Biol* **346:**967.

Xiu X, Puskar NL, Shanata JA, Lester HA, and Dougherty DA (2009) Nicotine binding to brain receptors requires a strong cation-pi interaction. *Nature* **458:**534–537.

Zhong W, Gallivan JP, Zhang Y, Li L, Lester HA, and Dougherty DA (1998) From ab initio quantum mechanics to molecular neurobiology: a cation-π binding site in the nicotinic receptor. *Proc Natl Acad Sci USA* **95:**12088–12093.

Zhou M (1999) Molecular recognition at the transmitter binding site of the nicotinic acetylcholine receptor channel. Ph.D. Thesis, SUNY at Buffalo, Buffalo.

Zhou M, Engel AG, and Auerbach A (1999) Serum choline activates mutant acetylcholine receptors that cause slow channel congenital myasthenic syndromes. *Proc Natl Acad Sci USA* **96:**10466–10471.

Address correspondence to: Anthony Auerbach, 309C Cary Hall, South Campus, SUNY at Buffalo, Buffalo, NY 14214. E-mail: auerbach@buffalo.edu